



ACADEMIC  
PRESS

Available online at [www.sciencedirect.com](http://www.sciencedirect.com)

SCIENCE @ DIRECT®

Journal of Solid State Chemistry 176 (2003) 633–645

JOURNAL OF  
SOLID STATE  
CHEMISTRY

<http://elsevier.com/locate/jssc>

# Local many-electron states in transition metal oxides and their surface complexes with atomic and molecular oxygen

A.M. Tokmachev and A.L. Tchougréeff\*

*Karpov Institute of Physical Chemistry, 10 Vorontsovo pole, 105064 Moscow, Russia*

Received 11 February 2003; received in revised form 23 June 2003; accepted 14 July 2003

## Abstract

The local many-electron states in transition metal oxides (TMOs) are considered in the framework of the effective Hamiltonian of the crystal field (EHCF) method. The calculations are performed with use of the  $5 \times 5 \times 5$  clusters modeling TMOs with the rock salt crystal structure. The  $d-d$  excitation spectra are calculated and discussed with the aim of interpreting the experimental data on optical adsorption and electron energy loss spectra. The EHCF method is extended to account for the electron correlation in the  $d$ -shell and some electronic variables of ligands simultaneously. This approach is used to calculate the states of atomic and molecular oxygen on the surfaces of the TMOs. The possible role of geometric parameters of the adsorption complex is evaluated. The metal–oxygen distance and the exit of the metal ion from the surface plane are varied in a wide range. In the case of molecular oxygen different coordination forms are considered and for all adsorption systems the weights of different oxygen states (triplet, singlet, and charge transfer) are estimated.

© 2003 Elsevier Inc. All rights reserved.

*Keywords:* Effective crystal field; Transition metal oxides;  $d-d$  spectra; Oxygen adsorption

## 1. Introduction

Transition metal oxides (TMOs) are important for numerous reasons. These range from catalytic activity in oxygenation processes [1] to superconductivity [2] of some TMO-based materials. These unique properties of oxides are determined by their electronic structure. In this paper we analyze theoretically the pitfalls occurring throughout the description of the local  $d$ -states in the TMOs and relate this to analysis of some experimental data on the spectral properties of transition metal ions in oxides based on optical adsorption (OA) and electron energy loss spectroscopy (EELS). Information on the energy spectrum of the  $d$ -shell is of no direct use in chemistry. However, it can be shown that catalytic properties of the surface transition metal ions are governed by mixing of the electronic states of the catalyst's  $d$ -shell and those of reactants/products. So we give a sketch of the corresponding theory of potential energy surface (PES) of chemical transformation taking place in the coordination sphere of a transition metal

ion (TMI). This analysis demonstrates how the ground state PES of a catalytic transformation depends on the weights of the excited and ionized states of the free reactants/products in it. Then a numerical analysis of the composition of the ground states of oxygen and dioxygen adsorbed by TMO surfaces is performed.

## 2. Cluster approximation for analysis of $d-d$ excitations in transition metal oxides

The electronic structure of the TMOs was extensively studied both experimentally and theoretically ([3–8] to mention a few). The spectrum of low-lying excitations controls the properties of TMOs: indeed [9] the relative energies of excitations  $d^n d^n \rightarrow d^{n+1} d^{n-1}$  and  $d^n \rightarrow L^\pm d^{n\pm 1}$  are set as a basis for classification of the oxides to Mott–Hubbard or charge-transfer insulator (MHI and CTI, respectively). This picture ignores other sets of important excited states which are possible in oxides. According to Ref. [4] (and references therein) the electronic states of TMOs with partially filled  $d$ -shells can be presented as band states of an ionic insulator (like MgO or CaO) supplied with the local multiplets of

\*Corresponding author.

E-mail address: [andrei@cc.nifhi.ac.ru](mailto:andrei@cc.nifhi.ac.ru) (A.L. Tchougréeff).

the  $d$ -electrons. Excitations inside the  $d$ -shell are responsible for the structure of optical spectra [5]. Namely these excited states—crystal field (CF)—excitations of the order of 1–3 eV shape the properties of TMOs on this energy scale. Meanwhile the excitations characteristic for the MHIs lay in the TMOs at 10 eV and higher and those characteristic for CTIs above 5 eV (We do not mention the gapless delocalized magnetic excitations—magnons—which are also characteristic for TMOs being antiferromagnets).

Phenomenological model for the spectrum of the CF excitations dates back to Bethe [10] and is known as crystal field theory (CFT). In the octahedral environment occurring in the above-cited TMO all having the rock salt crystal structure it is characterized by three empirical parameters  $A$ ,  $B$ , and  $C$  of which the first describes the energy splitting of one-electron  $d$ -levels and the other two, the Coulomb interaction of electrons in the  $d$ -shell. To improve the fitting of experimental spectra additional orbital-deformation parameters  $\lambda_e$  and  $\lambda_t$  are frequently introduced (for reference see [11,12]). The general feature of all CFT implementations and extensions is that the parameters mentioned above are considered as purely empirical. They cannot be evaluated in the frame of the CFT itself since no real description of the surrounding of the TMI is provided in its context except symmetry.

Thus there arises a problem of obtaining quantum chemical estimates for parameters of  $d$ - $d$  excitations in TMOs. Two major obstacles must be mentioned here. First, the TMOs are of course infinite three-dimensional objects pertaining to the realm of solid-state theory for which the account for the translational symmetry is indispensable. Second, the strong correlations of electrons in the  $d$ -shells are equally characteristic for TMOs as they are for other transition metal complexes. These correlations lead to problems for the self-consistent field (SCF)-based methods when the latter are applied to spin and symmetry properties of the ground state of the transition metal complexes and to their  $d$ - $d$  electron spectra. In fact, the single Slater determinant is poor even as a zero approximation to the structure of the ground state multiplet and electron correlation must be included explicitly—as a part of the wave function construct—to obtain correct results. Constructing the configuration interaction (CI) series based on the SCF orbitals does not solve the problem completely since they require a large number of configurations (most of them are to compensate the errors induced by the SCF approach at earlier stages of calculation) and converge slowly. Even more, when the solid state and correlation aspects “collide” in TMOs the result is completely disastrous: the one-electron band theory (the translation invariance compatible version of the SCF approximation) when applied to TMOs like MnO, CoO, and NiO predicts them to be partially filled  $d$ -band metals in

sharp contrast with experiment (see [3,4,11] and references therein). Such a result perfectly shows how far the SCF description may be from the real state of things even in highly symmetric systems, simple in many other respects.

The general opinion in the literature is that the required quantum chemical estimates can be obtained with use of the cluster approximation, i.e., by replacing the whole infinite three-dimensional crystal by the closest surrounding of the TMI in question. The general argument here is that the  $d$ -states are highly localized and thus their properties are controlled only by their closest surrounding—the first coordination sphere. This argument seems to be somewhat superficial, however. It is well known from optical absorption (OA) spectroscopy of molecular transition metal complexes that for the same set and spatial arrangement of donor atoms around the TMI the OA spectrum (and even the ground state) may become different if sufficient changes are chemically introduced to the peripheral groups of bulk organic ligands. The source of such a mutability is not of course any direct interaction between the peripheral groups and the TMI, but the chemically induced variations in those electronic structure parameters (ESPs) of the ligands which ultimately control the state of the  $d$ -shell. Thus we see that the local character of the  $d$ -states does not suffice by itself to justify the cluster approach and somewhat more elaborated treatment is necessary.

An appropriate method for analysis of the parameters of the  $d$ -shells in transition metal compounds is that of the effective Hamiltonian of the crystal field (EHCF) one proposed about a decade ago [13]. It allows to estimate the otherwise phenomenological  $A$  parameter of the CFT provided a reasonable description of the ESPs of the ligands is given. The EHCF methodology is based on the following features of electronic structure of transition metal complexes: (i) the presence of localized electrons in the open  $d$ -shell of transition metal atom, (ii) strong electron correlations inside  $d$ -shell and (iii) only small amount of electron transfer between  $d$ -shell and the ligands. All these features were implemented by using the combination of McWeeny group function [14] and effective Hamiltonian (Löwdin partition) [15] techniques and are based on subdividing the system into parts—correlated  $d$ -shell, effective Hamiltonian of which is treated on the full CI level and the rest (ligands) described in the semiempirical one-electron (SCF, single determinant) approximation. These moves allowed also to construct a successful numerical scheme reproducing experimental  $d$ - $d$  spectra of transition metal complexes with acceptable accuracy (the spin and symmetry properties of the ground and low-lying excited states are always correct and the errors in the determination of excitation energies are usually less than 1000  $\text{cm}^{-1}$ ) [16]. This method was implemented in several incarnations

depending on particular procedures employed to estimate the ligands' electronic structure parameters (ESPs, see below). The widest testing was done for the CNDO estimates of the ligands' ESPs [16], but the attempts using the INDO [17], SINDO1 [18], and MINDO/3 [19] also were quite successful.

According to the EHCF approach the matrix elements of the CF are dominated by the covalent contribution which actually takes into account the possibility of one-electron hopping between the  $d$ -shell and the ligands. In the form appropriate for the subsequent analysis they may be written as [20]

$$W_{\mu\nu}^{\text{cov}} = - \sum_i \beta_{\mu i} \beta_{\nu i} [G_{ii}^{\text{ret}}(I_d) + G_{ii}^{\text{adv}}(A_d)], \quad (1)$$

where  $\beta_{vi}$  are one-electron hopping integrals between the atomic  $d$ -state  $|v\rangle$  and the MO  $|i\rangle$  of the ligands. The Green functions contain all the information about the electronic structure of the ligands:

$$\begin{aligned} G_{ii}^{\text{ret}}(z) &= \langle \Phi_l | a_i (F_l^{\text{eff}} - z)^{-1} a_i^\dagger | \Phi_l \rangle, \\ G_{ii}^{\text{adv}}(z) &= - \langle \Phi_l | a_i^\dagger (F_l^{\text{eff}} - z)^{-1} a_i | \Phi_l \rangle, \end{aligned} \quad (2)$$

where  $F_l^{\text{eff}}$  is the self-consistent one-electron (Fock) operator for the ligands and  $\Phi_l$  is the single-determinant wave function for their electrons. The poles of Green's functions are the ionization potentials and electron affinities which in a line with the SCF approximation and the Koopmans' theorem are given in terms of the corresponding orbital energies  $\varepsilon_i$ :

$$\begin{aligned} I_i &= -\varepsilon_i - g_{di}, \\ A_i &= -\varepsilon_i + g_{di}. \end{aligned} \quad (3)$$

Formally, the difference between "molecular" and "crystal" forms of the EHCF theory should be minimal and the latter appears simply by replacing the MOs by the band (Bloch) states:

$$W_{\mu\nu}^{\text{cov}} = - \sum_n \sum_{\mathbf{k}} \beta_{\mu n\mathbf{k}} \beta_{\nu n\mathbf{k}} [G_{n\mathbf{k}}^{\text{ret}}(I_d) + G_{n\mathbf{k}}^{\text{adv}}(A_d)], \quad (4)$$

where  $\mathbf{k}$  is the wave vector in the  $n$ th band for the ground state of the insulating crystal like CaO and  $\beta_{\nu n\mathbf{k}}$  are one-electron hopping integrals between the atomic  $d$ -state  $|v\rangle$  and the Bloch band state  $|n\mathbf{k}\rangle$ . The above expression formalizes the picture by Harrison with the TMI multiplets immersed in the insulator band structure.

Both in the molecular and in the solid-state contexts the summation over all one-electron eigenstates of the ligands (the  $|i\rangle$  MO states or the Bloch states  $|n\mathbf{k}\rangle$ ) must be performed in Eq. (4). On the other hand it is clear that only the states (say AOs) located at the nearest-neighbor atoms have nonvanishing one-electron hopping integrals with the  $d$ -shell of interest. This allows [20] to rewrite the matrix elements of the CF Eq. (1) in a

local form:

$$W_{\mu\nu}^{\text{cov}} = - \sum_{LL'} \beta_{\mu L} \beta_{\nu L'} [G_{LL'}^{\text{ret}}(I_d) + G_{LL'}^{\text{adv}}(A_d)], \quad (5)$$

where

$$G_{LL'}^{\text{ret}}(z) = \sum_i \langle L|i\rangle G_{ii}^{\text{ret}}(z) \langle i|L'\rangle. \quad (6)$$

The local states relevant for the solid-state context are the Wannier states [21] defined by

$$|L\rangle = |w_n(\mathbf{R})\rangle = \frac{1}{\sqrt{V}} \sum_{\mathbf{k}} \exp(i\mathbf{k}\mathbf{R}) |n\mathbf{k}\rangle, \quad (7)$$

$$\mathbf{R} = \mathbf{r} + \mathbf{t}_x$$

for each (simple) band  $n$  and for each site  $\mathbf{r} + \mathbf{t}_x$  in the lattice where integer 3-vectors  $\mathbf{r}$  enumerate the unit cells of the crystal and the vector  $\mathbf{t}_x$  indicates the position of the  $x$ th atom in it. It was shown [22,23] that the Wannier states in the insulators decay exponentially while going away from the atom at  $\mathbf{r} + \mathbf{t}_x$  they are located at. So the summation in Eq. (5) is extended to the Wannier states located at the nearest-neighbor atoms of the TMI in question.

At a first glance this justifies applying the cluster approximation to the calculation of the states of the  $d$ -shells interacting with the band states of an ionic insulator. The things are, however, not so simple since the band structure of the solid manifests itself in the system of the poles of the corresponding Green's functions. Indeed, as one can check the poles of Green's function matrix elements in the local representation fill the whole range of energies which is spanned by the crystal band. In certain sense we face here the standard quantum mechanical situation: the things localized (measured) in one representation may not be localized in another one (for highly pedagogical discussion of this point see the book by Roald Hoffmann [24]). The Wannier states which are local in the coordinate (or site) representation are not local in the energy representation like the Bloch states are local in energy (they are the eigenstates of the corresponding Fock operator) and are not local in the coordinate (or site) representation and the question is to what extent this important feature of the real three-dimensional crystal is reproduced by the cluster calculation.

Thus, we see that the cluster calculations to be used to estimate the  $d$ - $d$  spectra are subject to a very strong condition: they have to reproduce somehow the effect of the whole set of band states. The last requirement in fact is not strictly bound to the EHCF framework within which it has been just formulated and applies irrespective of the specific technique used for numerical modeling the solid with use of a cluster. In view of the above analysis the case of minimal size clusters  $MO_n^{2(n-1)-}$  [25–28] seems to be the most suspicious. In the crystals with the rock salt structure the filled

band states of the  $e_g$  symmetry mostly formed by the  $2pO$ -states contribute to the splitting of the  $d$ -orbitals. In the case of minimal cluster only one state (MO) of this symmetry is provided by the ligands. Correspondingly Green's function has only one pole at the corresponding orbital energy value. A simple analysis shows that in a three-dimensional rock-salt-type solid at least two states of the  $e_g$  symmetry appear from each band at each energy value in the latter. The number of poles is corresponding, i.e., infinite, spanning the whole range of the respective energy bands. Generally, one pole is not enough to reproduce the whole band with a nonzero width. In an empirical approach one could of course tune an energy of a single level in order to mimic the effect of the band, but on an ab initio level precisising the absolute position of the  $e_g$ -state energy in the cluster can spoil the results on the splitting in the crystal since the exact energy of this state can become far from the position most effective for reproducing the interaction of the  $d$ -shell with the band.

We see that the key drawback of the minimal cluster models is the meagerness of the available spectrum of one-electron states on the ligands. On the other hand the role of the Madelung potential whose importance for accessing the sensible results on  $d$ -shell splitting in the minimal cluster approximation is frequently stressed [27,29] seems to be overestimated. Of course taking the Madelung potential is important in order to reproduce correctly the relative positions of the diagonal matrix elements of the ligands' Fock operator on the energy scale. This in its turn is important for determining the width of the valence band, the charge distribution and other ligand-related ESPs affecting the splitting, but by itself the Madelung potential only weakly influences the splitting of the  $d$ -shell since it is almost spherically symmetric. Indeed, our calculations show that the contribution of the charges beyond the first coordination here (six charges) to the splitting of the  $d$ -states constitute only 3% per unit charge.

It is interesting to notice that the Madelung potential is sometimes implicitly used within otherwise ab initio procedures as a fitting parameter serving to improve the result. It is usually estimated with use of the formal charges of the ions in the lattice. The effective charges of ions can be, however, far from the formal ones due to electron delocalization (band formation) in the crystal. For example, it was estimated that the charges in the KCl are approximately only halves of the formal ones [4]. This effect is also very poorly reproduced by the minimal cluster models due to lack of the translational symmetry. In the minimal cluster calculations the effective charges residing, respectively, on the metal and the oxygen are always different. For all these reasons we incline to an opinion that the reasonable agreement between experimental data and ab initio

minimal cluster calculations (particularly those which contain implicit adjustment schemes beyond otherwise strict ab initio procedures) is an accidental coincidence.

The intrinsic drawbacks of the minimal cluster models can be reduced by increasing the size of the cluster since (i) the molecular orbitals of the larger clusters are closer to the band states of the solid and (ii) the atomic charges obtained are closer to the exact ones. The strong dependence of band gaps on the cluster size was demonstrated on the example of MgO and KCl clusters [30] in the small size range.

### 3. Method of effective Hamiltonian for reaction centers

Knowledge of electronic structure of the TMOs is important since it controls their chemical properties including catalytic activity in oxygenation processes [1]. In the absence of a catalyst these processes are restricted due to spin conservation rules. It is usually believed that the  $d$ -shell of a TMI serves as an electron donor or acceptor for the reactants [31]. Also, interactions between catalyst and reactants can change their spin states getting around the spin conservation restriction without significant charge transfer [32]. All this testifies that the electron correlation in the  $d$ -shell and reactants of catalytic transition metal complex (complex formed by catalyst and reactants coordinated to it) must be taken into account simultaneously. The situation in general can be described phenomenologically [33,34]. The Hamiltonian for the entire catalytic complex is a sum of those for the free subsystems (catalyst and reactants/products) and of their interaction:

$$H = H_{\text{cat}} + H_{\text{react}} + H_{\text{int}}. \quad (8)$$

Each free subsystem is completely characterized by its spectrum of electronic states. The wave function of the whole system is a linear combination of all possible antisymmetrized products of these states:

$$\Phi_{\text{whole}}^0 = \sum_{ij} c_{ij}^0 \Phi_{\text{cat}}^i \wedge \Phi_{\text{react}}^j, \quad \sum_{ij} (c_{ij}^0)^2 = 1 \quad (9)$$

with a restriction that the total number of electrons in all product functions is the same. Note that such a form of the electronic state is precisely what is nowadays called the "entangled state" in the context of quantum measurement theory. The electronic energy calculated with wave function (9) has the form:

$$E_{\text{el}} = \sum_{ij} (c_{ij}^0)^2 (E_{\text{cat}}^i + E_{\text{react}}^j) + \sum_{ij} \sum_{i'j'} c_{ij}^0 c_{i'j'}^0 \times \langle \Phi_{\text{cat}}^i \wedge \Phi_{\text{react}}^j | H_{\text{int}} | \Phi_{\text{cat}}^{i'} \wedge \Phi_{\text{react}}^{j'} \rangle. \quad (10)$$

This expression contains amplitudes of different product states in the expansion of the ground state of the whole system. The perturbative estimates for these

amplitudes are:

$$c_{ij}^0 \propto \frac{\langle \Phi_{\text{cat}}^i \wedge \Phi_{\text{react}}^j | H_{\text{int}} | \Phi_{\text{cat}}^0 \wedge \Phi_{\text{react}}^0 \rangle}{E_{\text{cat}}^i - E_{\text{cat}}^0 + E_{\text{react}}^j - E_{\text{react}}^0}. \quad (11)$$

The  $c_{ij}^0$  amplitudes can be also estimated through a standard variational procedure provided the parameters of the phenomenological Hamiltonian Eq. (8) are given. With them the expression, Eq. (10), becomes an explicit formula giving the PES of a chemical transformation occurring with ligands coordinated to the catalyst. It is clearly a superposition of various PESs of different electronic states of the reactants/products which are mixed together. The detailed description of how this formula for the PES explains the catalytic action and allows to correlate physical properties of the free catalyst which are controlled by its energy spectrum  $E_{\text{cat}}^i - E_{\text{cat}}^0$  with the catalytic activity is given in [33,34].

In fact the EHCF method [13] is designed to be a tool providing the estimates for the CF phenomenological Hamiltonian. Though it does not directly apply to the problem of catalysis since it assumes the number of electrons in the  $d$ -shell to be a good quantum number (i.e., integer—equal to the number of  $d$ -electrons in the free transition metal ion—and constant) and the ligands wave function to be one of the ground state the same principles can be used to construct the effective Hamiltonian for the electron variables describing the  $d$ -shell and carefully chosen part of those in the ligands. In the case of chemical process it is usually possible to choose a small subset of orbitals responsible for the transformation. The structure of these orbitals and/or their occupation numbers significantly change in the course of reaction. We combine these orbitals into the  $r$ -subsystem (reactive one). For example, the isomerization of quadricyclane to norbornadiene is a rearrangement of four-membered ring into two double bonds. This reaction is forbidden according to the Woodward–Hoffmann rules [35] since the HOMO and LUMO of  $b_1$  and  $b_2$  symmetry of quadricyclane and norbornadiene invert their occupancies in the course of isomerization. Therefore, these two orbitals must be considered as active and must be included into the  $r$ -subsystem. In the case of atomic oxygen adsorption  $p_x$  and  $p_y$  atomic orbitals of oxygen bearing unpaired electrons must be included into the  $r$ -subsystem since the electrons on these orbitals determine the spin symmetry of the oxygen state and are responsible for adding electrons to and removal from the oxygen atom. Analogously, in the case of molecular oxygen adsorption, the degenerate  $\pi^*$  orbitals with unpaired electrons constitute the  $r$ -subsystem. In general, using some number of highest occupied and some number of lowest unoccupied molecular orbitals is a safe choice for the  $r$ -subsystem. Of course this recommendation is of little value for someone who is interested in numerical result only and

can also afford large-scale CIs. Our concern here is largely to develop a semiquantitative tools supporting qualitative understanding and explanation of catalysis phenomenon in intuitively transparent terms.

To consider the transition metal complex with chemically active ligands we divide the system in two parts: the first part (requiring correlated description) is a combination of the  $d$ -shell and the  $r$ -subsystem. It is denoted as  $d \oplus r$  and is assumed to be described on the full CI level. The second part (environment) is presented by all the ligands without those (molecular) orbitals of reactants which are included into the  $r$ -subsystem. It is denoted as  $l \ominus r$  and is described in the SCF approximation. The separation of the complex into above parts implies also the subdivision of the Hamiltonian:

$$H = H_{d \oplus r} + H_{l \ominus r} + V'_c + V'_R, \quad (12)$$

where  $V'_c$  and  $V'_R$  are operators of the Coulomb and resonance interaction between the subsystems  $d \oplus r$  and  $l \ominus r$ . (Here we omit the two-electron transfers which are generally thought to be very small.) The numbers of electrons in the subsystems are assumed to be fixed and the wave function is taken as the antisymmetrized product of the wave function of the  $d \oplus r$ -subsystem and the ground state wave function of the  $l \ominus r$ -subsystem. So, the effective Hamiltonian for the  $d \oplus r$ -subsystem should be constructed by using the projection  $P$  on the space with the assumed numbers of electrons in the subsystems. This effective Hamiltonian is obtained by averaging the effective Hamiltonian over the wave function of the  $l \ominus r$ -subsystem:

$$H_{d \oplus r}^{\text{eff}} = H_{d \oplus r} + \langle\langle V'_c + V'_{RR} \rangle\rangle, \quad (13)$$

where the resolvent contribution  $V'_{RR}$  couples two electron transfers between subsystems in such a way that the numbers of electrons in the subsystems are left intact:

$$V'_{RR} = P V'_R Q (EQ - QH_0 Q)^{-1} Q V'_R P, \quad (14)$$

where  $H_0$  is the part of the total Hamiltonian diagonal with respect to the operators  $P$  and  $Q (= 1 - P)$ , i.e., the total Hamiltonian without electron transfers between subsystems. The dependence of the resolvent operator on the energy is rather weak and can be omitted. This corresponds to the second order of the operator form of the Rayleigh–Schrödinger perturbation theory.

The wave function of the ligands ( $l$ -subsystem) is given by the antisymmetrized product of the molecular orbitals obtained by an SCF procedure applied to the ligands' Hamiltonian. After this some of the orbitals are ascribed to the  $r$ -subsystem while the rest forms the  $l \ominus r$ -subsystem and is used for averaging in Eq. (13).

The most important part is a construction of the effective Hamiltonian for the  $d \oplus r$ -subsystem [36]. After it is constructed the electronic energy of the  $k$ th state of the whole complex can be found as a sum of two

averages:

$$E^k = \langle \Psi_{d\oplus r}^k | H_{d\oplus r}^{\text{eff}} | \Psi_{d\oplus r}^k \rangle + \langle \Psi_{l\ominus r} | H_{l\ominus r} | \Psi_{l\ominus r} \rangle, \quad (15)$$

i.e., the differences of eigenvalues of the effective Hamiltonian for the  $d\oplus r$ -subsystem correspond to the spectrum of the whole system.

We give now the explicit form of the effective Hamiltonian Eq. (13). It is a sum of one- and two-electron contributions:

$$H_{d\oplus r}^{\text{eff}} = H_{d\oplus r}^{(1)} + H_{d\oplus r}^{(2)}. \quad (16)$$

The one-electron contribution is a sum of five contributions:

$$H_{d\oplus r}^{(1)} = \sum_{\mu \in d} H_{d\oplus r}^{(1)\text{at},\mu\mu} + \sum_{\mu, \nu \in d} H_{d\oplus r}^{(1)\text{ECF},\mu\nu} + \sum_{\substack{\mu \in d \\ i \in r}} H_{d\oplus r}^{(1)\text{res},\mu i} \\ + \sum_{i \in r} H_{d\oplus r}^{(1)\text{int},ii} + \sum_{i,j \in r} H_{d\oplus r}^{(1)\text{dint},ij}. \quad (17)$$

The first one is the Coulomb interaction of  $d$ -shell electrons with the core and electron density populating the  $s$ - and  $p$ -orbitals of transition metal atom. It has the form:

$$H_{d\oplus r}^{(1)\text{at},\mu\mu} = \sum_{\sigma} d_{\mu\sigma}^+ d_{\mu\sigma} \left( U_{dd} + P_{ss} g_{sd} + \bar{g}_{pd} \sum_{i \in p} P_{ii} \right), \quad (18)$$

where  $P_{ii}$  is the diagonal element of the density matrix of the  $l\ominus r$ -subsystem for  $s$ - and  $p$ -orbitals of transition metal ion. The next contribution to Eq. (17) is the crystal field induced by the ligands. Its form coincides with that of the ECF method [13]:

$$H_{d\oplus r}^{(1)\text{ECF},\mu\nu} = \sum_{\sigma} d_{\mu\sigma}^+ d_{\nu\sigma} \left[ \sum_L (P_L - Z_L) V_{\mu\nu}^L \right. \\ \left. - \sum_{j \in l\ominus r} \beta_{\mu j} \beta_{\nu j} \left\{ \frac{1-n_j}{\Delta E_{dj}} - \frac{n_j}{\Delta E_{jd}} \right\} \right], \quad (19)$$

where the first expression in square brackets is the Coulomb interaction of the  $d$ -shell with the ligands averaged over wave function of the  $(l\ominus r)$ -subsystem. Here  $V_{\mu\nu}^L$  denotes the matrix element of such interaction and  $P_L$  is the electron density on the ligand atom  $L$  due to electrons of the  $(l\ominus r)$ -subsystem. This contribution corresponds to the ionic model for the splitting of the  $d$ -levels when it is caused only by the interaction with charges on the ligand atoms. The second contribution to Eq. (19) arises from the resolvent operator Eq. (14). The  $\beta_{\mu j}$  is the corresponding resonance integral;  $n$  is the occupancy of the orbital (it equals to 1 if it is doubly occupied and zero otherwise);  $\Delta E_{dj}$  and  $\Delta E_{jd}$  are the energies of the one-electron transfer from the  $d$ -shell to the  $j$ th molecular orbital and vice versa. It is important to say that the calculation of electron transfer energies

explicitly takes into account the difference between the ionization potential and the electron affinity for the  $d$ -shell due to the Coulomb interaction between  $d$ -electrons. Taking into account this interaction in the problem of description of local electron group interacting with bands was demonstrated in Ref. [37]. This contribution to the  $d$ -shell splitting can be characterized as the covalent one.

The next contribution to the one-electron part Eq. (17) describes one-electron transfers between the  $d$ -shell and the active orbitals belonging to the  $r$ -subsystem. This operator is responsible for variations of the occupation numbers for the  $d$ -shell and the  $r$ -subsystem:

$$H_{d\oplus r}^{(1)\text{res},\mu i} = -\beta_{\mu i} \sum_{\sigma} (d_{\mu\sigma}^+ r_{i\sigma} + r_{i\sigma}^+ d_{\mu\sigma}). \quad (20)$$

The fourth contribution to the one-electron energy arises from the  $r$ -subsystem only. It can be expressed through the orbital energies of the  $r$ -subsystem  $\varepsilon_i$  obtained in the SCF calculation of the  $l$ -subsystem:

$$H_{d\oplus r}^{(1)\text{int},ii} = \left[ \varepsilon_i - \sum_{j \in r} n_j (2J_{ij} - K_{ij}) \right] \sum_{\sigma} r_{i\sigma}^+ r_{i\sigma}, \quad (21)$$

where  $J_{ij}$  and  $K_{ij}$  are the Coulomb and exchange integrals between the  $i$ th and  $j$ th molecular orbitals. The last contribution to the one-electron part of the effective Hamiltonian is

$$H_{d\oplus r}^{(1)\text{dint},ij} = -n_d G_{dij} \sum_{\sigma} r_{i\sigma}^+ r_{j\sigma}, \quad (22)$$

where  $G_{dij}$  is the matrix element ( $dd | ij$ ).

Two-electron contributions are of three different types:

$$H_{d\oplus r}^{(2)} = \sum_{\mu, \nu, \rho, \eta \in d} H_{d\oplus r}^{(2)\mu\nu\rho\eta} + \sum_{\substack{\mu \in d \\ i, j \in r}} H_{d\oplus r}^{(2)\mu ij} + \sum_{i, j, k, l \in r} H_{d\oplus r}^{(2)ijkl}, \quad (23)$$

where

$$H_{d\oplus r}^{(2)\mu\nu\rho\eta} = \frac{1}{2} (\mu\nu | \rho\eta) \sum_{\sigma\tau} d_{\mu\sigma}^+ d_{\nu\tau}^+ d_{\rho\sigma} d_{\eta\tau}, \\ H_{d\oplus r}^{(2)\mu ij} = G_{\mu ij} \sum_{\sigma\tau} d_{\mu\sigma}^+ d_{\mu\sigma} r_{i\tau}^+ r_{j\tau}, \\ H_{d\oplus r}^{(2)ijkl} = \frac{1}{2} (ij | kl) \sum_{\sigma\tau} r_{i\sigma}^+ r_{k\tau}^+ r_{l\tau} r_{j\sigma}, \quad (24)$$

where the standard notation for the Coulomb matrix elements is used. The number of one-electron states in the  $d\oplus r$ -subsystem is rather small (seven in the case of atomic or molecular oxygen adsorption on the surface of the TMO). It makes feasible the calculation of the eigenvalues and eigenstates of the effective Hamiltonian Eq. (13) by the full configuration iteration procedure. To this purpose the unitary group approach was used [38] allowing for the construction of the spin-adapted

many-electron basis functions and the necessary elementary generators.

## 4. Results and discussion

### 4.1. EHCF for the *d*-shells in TMOs and *d*–*d* spectra

In order to substantiate our reasoning given above we performed calculations of the parameters of the CF affecting the *d*-shells of TMIs in the corresponding oxides by the EHCF method and of the spectra of *d*–*d* excitations for TMIs in the different positions inside the TMOs clusters with use of the EHCF estimated parameters. The structures of the clusters were taken from the X-ray experiments for the bulk. Therefore, the reconstruction of the crystal lattice near the surface was not taken into account. We also did not change any parameters specially for the TMOs. So, the Racah parameters *B* and *C* were taken the same as in the free ion. The Burns' exponents for the metal *d*-orbitals were used and the resonance parameters  $\beta^{M-O}$  were taken equal to those fitted to reproduce the spectra of the hexaaquacomplexes  $[M(H_2O)_6]^{2+}$  [39].

Previously we studied the dependence of the EHCF results on the cluster size. In Refs. [28,40] a series including the minimal cluster  $MO_6^{10-}$  and the cubic clusters representing fragments of the oxide structure— $M_{13}O_{14}^{2-}$ ,  $M_{32}O_{32}$ , and  $M_{63}O_{62}^{2+}$  ( $3 \times 3 \times 3$ ,  $4 \times 4 \times 4$ , and  $5 \times 5 \times 5$  atoms in the cluster, respectively) has been calculated. The relevant data are given in Table 1. The non-stoichiometry of  $3 \times 3 \times 3$  and  $5 \times 5 \times 5$  clusters can influence the absolute positions of one-electron levels in the ligand system and the *d*-shell. At the same time the formulation of the EHCF method requires only their differences. In this case the role of non-stoichiometry of cluster is rather small since the non-stoichiometry of the cluster leads to very close shifts of the energy levels. First of all one can notice that there exists a noticeable dependence of the calculated characteristics of the clusters with their size. One can see that the convergence in atomic charges is approximately achieved when the largest clusters in the series are used. It indirectly suggests that the MOs and the corresponding orbital energies of such a cluster sample the band states of the corresponding three-dimensional crystal with sufficient accuracy. In addition to a well-known dependency of the calculated charges which reaches approximately the bulk value for the  $5 \times 5 \times 5$  clusters we notice that the values of 10Dq vary nonmonotonously with increase of the cluster size at least for intermediate cluster sizes. In fact the values obtained for the minimal clusters  $MO_6^{10-}$  are systematically closer to the experimental values than those obtained for the  $3 \times 3 \times 3$  clusters. So we would come to a conclusion that in the case of the octahedral clusters of minimal size certain compensation of errors may take place. However, it is not clear whether the same should always happen and whether we may expect a reasonable result also for lower symmetry  $MO_5^{8-}$  clusters used to model the surface TMIs. Indeed, our calculation using minimal cluster [28] shows that in the case of the corresponding Co cluster the first excited state  ${}^4E$  has the energy 0.45 eV. This contradicts to the high-resolution EELS experiment [43] which positions this state at 0.05 eV. Use of  $5 \times 5 \times 5$  cluster allows to position this state correctly (0.03 eV in our calculation [40]). Meanwhile, it can be checked by detailed analysis of the contributions to the EHCF that the covalent contribution to the splitting between the lowest *e*- and the next in energy  $b_2$ -orbitals of the Co ion is overestimated by an order of magnitude in the minimal cluster calculation. This

Table 1  
Calculated charges and splittings for different cluster sizes

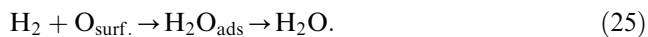
Oxide	Atom	Cluster size				Band gap (eV)	Ref.
		$[MO_6]^{10-}$	$3 \times 3 \times 3$	$4 \times 4 \times 4$	$5 \times 5 \times 5$		
NiO	Ni	1.06	0.82	0.82	0.85	11.82	[41]
	O	−1.84	−0.80	−0.85	−0.84		
	10Dq	0.81	1.04	0.90	0.87		
CoO	Co	1.02	0.86	0.87	0.90	11.25	[42]
	O	−1.84	−0.84	−0.89	−0.89		
	10Dq	0.88	1.03	0.93	0.90		
FeO	Fe	0.98	0.92	0.94	0.96	10.61	[3]
	O	−1.83	−0.89	−0.95	−0.96		
	10Dq	1.01	1.15	1.07	1.04		
MnO	Mn	0.93	0.98	1.01	1.03	9.71	—
	O	−1.82	−0.94	−1.01	−1.02		
	10Dq	0.94	0.90	0.86	0.84		

defect is lifted in the larger cluster calculation where this splitting is significantly reduced.

On the basis of the above result we conclude that applying the clusters of the size  $5 \times 5 \times 5$  would be a safer choice to be employed when the interactions between the surface TMI with an adsorbate is treated with use of the effective Hamiltonian technique. For the purpose of testing we consider the effect of NO adsorption on the (100) surface of NiO by the effective Hamiltonian approach for transition metal complexes with chemically transforming ligands. The  $r$ -subsystem is formed by two highest occupied orbitals of the NO molecule containing together three electrons. Let us consider the effect of NO adsorption on the  ${}^3E$  surface state of NiO. It is well established experimentally that the relative energy of this state increases by 0.33 eV during the adsorption [27]. When the VCI or MC-CEPA methods are applied to this process the shift obtained is 0.1 eV [27]. The shift of this level depends of course on the  $r(\text{Ni-N})$  distance and our calculations show that the experimental value is exactly reproduced for  $r(\text{Ni-N})=1.71 \text{ \AA}$ . This distance does not seem to be very short since it is known, for example, that the experimentally determined distance  $r(\text{Fe-N})$  in complexes with NO is usually in the range 1.70–1.75 Å.

#### 4.2. Oxygen adsorption at the TMO surfaces

In the previous subsection we considered the effective Hamiltonian description of the local excitations in the TMOs. The acceptable agreement between the calculated and experimental values in this case allows to hope that the adsorption on the TMOs will also be reproduced adequately. The TMOs and related materials are often used as oxidation catalysts in the processes of detoxication of organic substances or carbon oxide utilization. The mechanism of these reactions is not completely understood. It was experimentally shown that the activation energy in the reaction of the dihydrogen oxidation is proportional to the oxygen binding energy to the surface of the TMO [44]. This observation allowed to make a conclusion that the rate-determining step in this oxidation process is an interaction of dihydrogen with an oxygen atom adsorbed on the catalyst surface:



The reaction of dihydrogen with triplet oxygen is restricted. Thus, one can expect that the electronic structure of the oxygen changes significantly when it is adsorbed by the surface of the TMO catalyst. The experimental determination of the state of the adsorbed oxygen atom is problematic since it is difficult to distinguish between effects from the adsorbed oxygen atoms and those coming from the bulk of the oxide. In the literature there are indirect experimental data [45]

for oxygen atoms on the surface of NiO certifying that the contribution of the anion-radical form of the oxygen  $\text{O}^{\bullet-}$  is significant. The same conclusion was made on the ground of purely Coulomb estimations [46]. The electron spin resonance experiments unequivocally show that the anion-radical  $\text{O}^{\bullet-}$  is formed during adsorption of the oxygen on the surfaces of the TMOs. It has been concluded that the anion-radical oxygen form is highly active in the oxidation of carbon oxide and dihydrogen [47,48].

We calculated the oxygen states on the surfaces of the TMOs by the hybrid method of the electronic structure calculation for transition metal complexes with chemically active ligands described in details above. In all the cases the surface of the TMO was modeled by the  $5 \times 5 \times 5$  cluster and the oxygen  $2p_x$ ,  $2p_y$  orbitals with unpaired electrons constituted the  $r$ -subsystem. We studied the role of two structural parameters on the electronic state of the oxygen—the metal–oxygen distance and the exit of the transition metal ion from the surface plane modeling the reaction of the surface on the adsorption (see Fig. 1). The method gives the states of the  $d \oplus r$ -subsystem characterized by the amplitudes of the configurations given by their Young tableaux. Our aim is extracting the states of the adsorbed oxygen, i.e. of the  $r$ -subsystem. A set of Young tableaux corresponds to the definite state of the whole system but not to that of the  $r$ -subsystem. If two electrons are on the same orbital of the  $r$ -subsystem and other orbital is vacant the  $r$ -subsystem state is singlet. When both orbitals of the  $r$ -subsystem are singly occupied and belong to different columns of the Young tableau and the system has nonzero total spin the determination of the state of the  $r$ -subsystem is not so trivial. In this case the Young tableau of  $d \oplus r$ -subsystem contains a mixture of singlet and triplet states of the  $r$ -subsystem and to find the weights of the oxygen states the systems of two inhomogeneous linear equations must be solved. The necessary subduction coefficients were taken from Ref. [49].

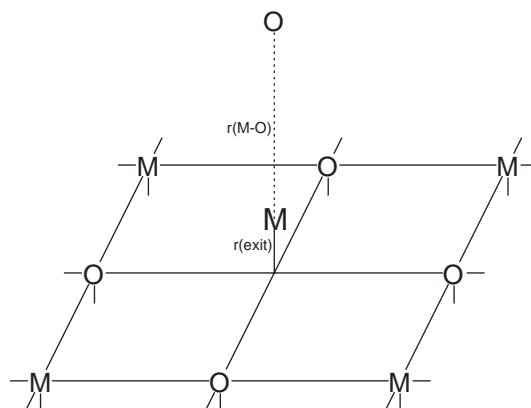


Fig. 1. Scheme of oxygen adsorption on the surface.

We choose the states map as a form of representation of the results on the adsorption. In principle, the EHCF method is capable of geometry optimization [50]. At the same time the geometry optimization gives the electronic state only in one point. When we construct the map we have more information since (a) relatively small error in the optimized geometry parameters can cause the incorrect result on the electronic state and, (b) perturbation by other molecules can cause the change of the electronic state. The states map for the atomic oxygen adsorbed on the (100) surface of FeO (dependence of the system's electronic state on the structural parameters) is given in Fig. 2. The interatomic distance Fe–O<sub>ads</sub> was varied in the range 1.2–2.4 Å while the exit of the metal atom from the plane was varied in the range 0.0–0.5 Å. The positions of the lines on the states map are given with precision of 0.01 Å. The weights of singlet ( $W(O^s)$ ) and charge-transfer (one electron from the  $d$ -shell to the  $r$ -subsystem,  $W(O^-)$ ) and the total charge on the oxygen ( $Q(O)$ ) are given for some representative points on the map. The same way of construction is used for other states maps (see below). In the most cases the position of the border between different states only slightly depends on the exit of the metal ion from the plane. It means that these transitions are mainly caused by the interaction of the  $d$ -shell with the adsorbed

oxygen atom. When the Fe–O distance is larger than 2.07 Å the state of the oxygen is almost totally triplet with small admixture of the anion form. The singlet state is totally absent. In the case of small values of  $r(\text{Fe-plane})$  the ground state is the  $^3E$  state obtained from the quintet state of the surface ion  $\text{Fe}^{2+}$  in the oxide and from the triplet state of the oxygen atom. The exit of the metal ion from the surface plane changes the state of the adsorption complex. The analogous change of the ground state can be obtained for the free TMO due to changes in the crystal field. At the same time in the case of adsorption these changes couple with crystal field modifications due to the oxygen atom that leads to the nontrivial form of the region  $^3A_2$  on the states map. For the intermediate distances  $r(\text{Fe-O})$  the ground state is the  $^5E$  state with noticeable weights of the singlet and anion states of oxygen. In the case of small distances  $r(\text{Fe-O})$  we can see the singlet and triplet states with relatively large weights of the singlet and charged forms of oxygen. Moreover, the weight of the doubly charged oxygen forms becomes noticeable. It should be noted that the changes of weights of different states are not monotonic. For example, the state  $^5A_1$  in a small region near 1.5 Å along the  $r(M-O)$  coordinate does not contain any singlet contribution at all, while its neighbor states contain about 20% of the singlet oxygen weight.

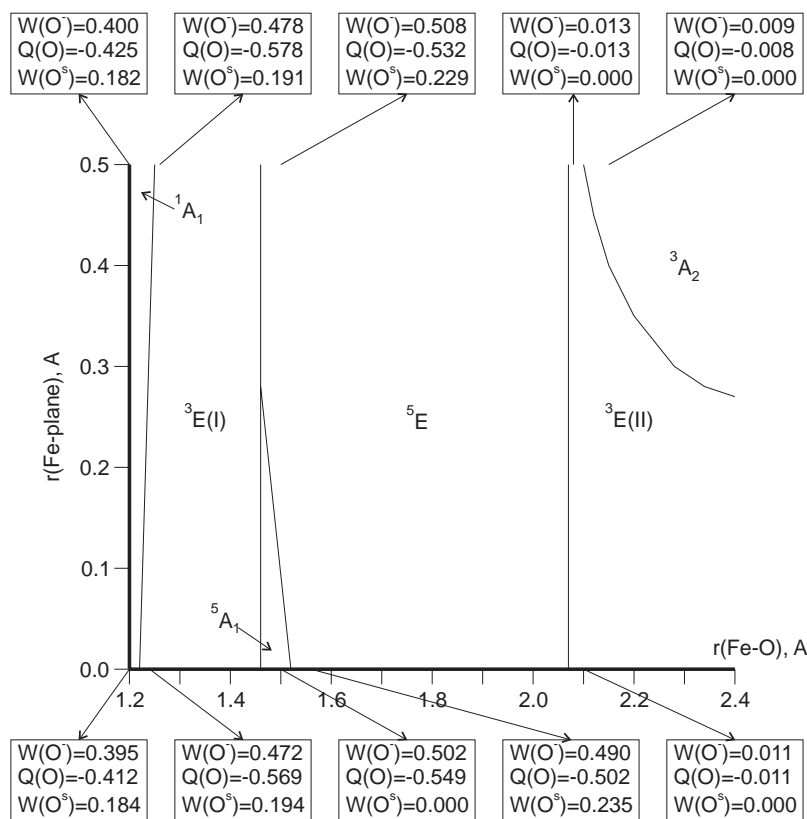


Fig. 2. Map for adsorption of atomic oxygen on FeO:  $W(O^-)$ —weight of the anion form of the oxygen;  $W(O^s)$ —weight of the singlet form of the oxygen;  $Q(O)$ —charge on the oxygen.

It is noteworthy that the exit of the metal ion from the surface plane usually does not change significantly the weights of different oxygen states if only the change of the state of the whole complex does not occur under this condition.

In the case of atomic oxygen adsorption on the surface of CoO the states map is somewhat simpler (Fig. 3). For large  $r(\text{Co-O})$  distances the ground state is the sextet ( ${}^6A_1$ ) mainly formed by the quartet ground state of the surface  $\text{Co}^{2+}$  ion in the oxide and by the triplet state of the oxygen atom. This state prevails on the states map. As in the case of FeO the anion form of the oxygen atom has significant weight for smaller and intermediate  $r(\text{Co-O})$  distances. At the same time the states with contribution from the singlet oxygen are almost absent on this map. The singlet oxygen appears only for the  ${}^2E$  state occurring at very small distances  $r(\text{Co-O})$  and for the  ${}^4E$  state which becomes the ground one only for large values of  $r(\text{Co-plane})$  and in a very small area of the map (Fig. 3). In the case of adsorption of atomic oxygen on the NiO surface the states map is very simple. The quintet state formed by the triplet states of the surface transition metal ion in the oxide and of the oxygen atom is the ground one for  $r(\text{Ni-O})$  exceeding  $1.38 \text{ \AA}$ . The singlet form of the oxygen atom appears nowhere on the map. The amount of charge

transfer between the oxide and the oxygen atom is quite similar to that obtained for adsorption on the CoO. In the case of atomic oxygen adsorption on the MnO the whole map is formed by only one quartet state mainly constructed from the sextet state of the oxide and the triplet state of the oxygen atom. The state of the  $d$ -shell conserves the structure of the ground state of the free  $\text{Mn}^{2+}$  ion ( ${}^6S$ ). The singlet oxygen can be found in noticeable quantity even for medium values of  $r(\text{Mn-O})$ . It should be noted that in the case of MnO the weight of charge-transfer states is somewhat smaller than that for other oxides.

It is interesting to compare the main features of the adsorption of atomic and molecular oxygen on the oxides. In the case of dioxygen adsorption the structure of the  $r$ -subsystem orbitals is determined in the Coulomb field of the oxide. There exists an opinion that the Coulomb field of the catalyst can change the spin state of the oxygen molecule from the triplet one to the singlet one [51]. At the same time the calculations show that this effect can be achieved only for unphysically large Coulomb fields. The molecular oxygen has more geometric degrees of freedom and the ionization potentials and electron affinities are somewhat different from those of the atomic oxygen. Moreover, in the case of molecular oxygen the vacant

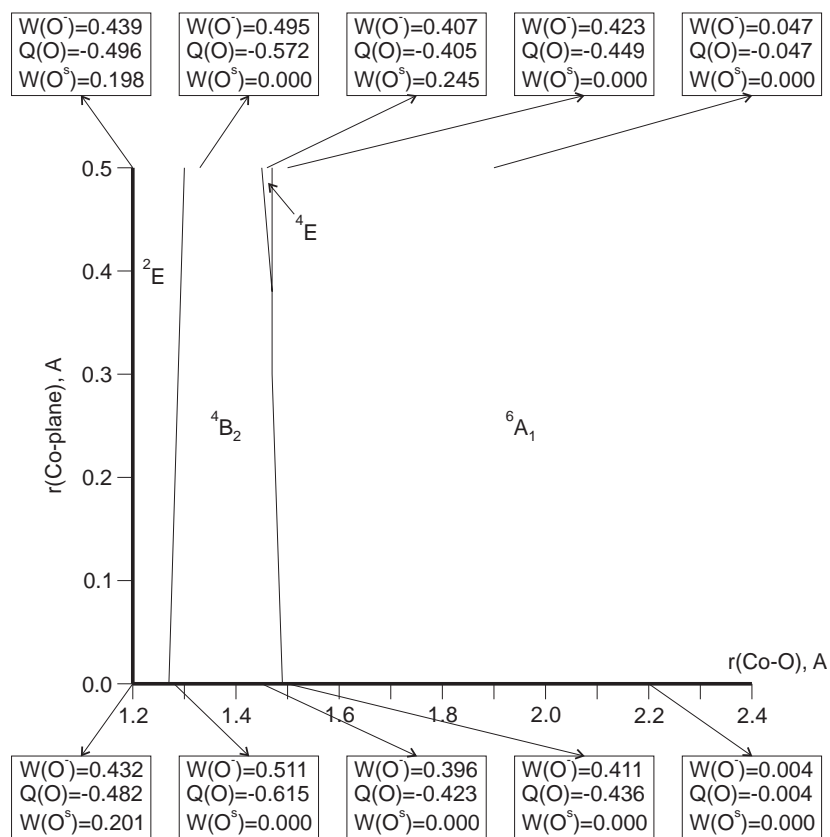


Fig. 3. Map for adsorption of atomic oxygen on CoO:  $W(\text{O}^-)$ —weight of the anion form of the oxygen;  $W(\text{O}^s)$ —weight of the singlet form of the oxygen;  $Q(\text{O})$ —charge on the oxygen.

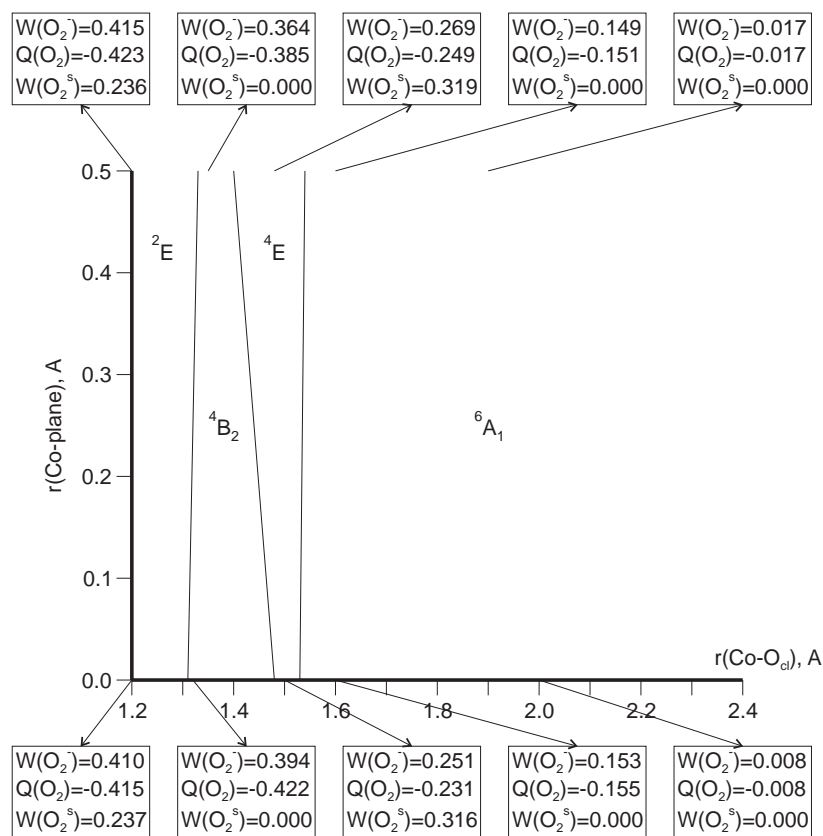


Fig. 4. Map for end-on adsorption of atomic oxygen on CoO:  $W(\text{O}_2^-)$ —weight of the anion form of the oxygen;  $W(\text{O}_2^s)$ —weight of the singlet form of the oxygen;  $Q(\text{O}_2)$ —charge on the oxygen.

orbitals can be important. It obviously affects the electronic structure of the adsorption complex. We present here the states maps for two structures of molecular oxygen adsorption on the (1 0 0) surface of CoO—the end-on one (Fig. 4) and the side-on one (Fig. 5). In the case of the end-on adsorption one can see that the general features of the states map representing adsorption of atomic oxygen (Fig. 3) are conserved (including the origin of the states and the positions of border lines between them) except the width of the region of the  $^4E$  state. It certifies that the changes of the states are mainly caused by the crystal field induced by the doubly occupied orbitals of the closest oxygen atom. The change of the atomic oxygen by the molecular one leads to relatively small changes in the weights of different configurations for equivalent points on the map. At the same time there are some general trends: this change leads to decreasing of the weight of the anionic oxygen and to increasing the weight of the singlet states of the oxygen species. In the case of side-on adsorption the map differs significantly from that for the end-on adsorption mainly due to difference in the symmetry of the adsorption complex. It is noteworthy that significant weight of singlet oxygen can be found in this case even for relatively large interatomic distances. This form of adsorption is also more effective for

formation of negatively charged oxygen species. Moreover, for small interatomic distances  $r(\text{Co}-\text{O})$  the doubly charged oxygen has significant weight—more than 8%.

## 5. Conclusions

We considered the problem of constructing local many-electron states in the TMOs and estimating their relative energies. The important statement here is that the correlated approximation of the  $d$ -shell electronic structure is necessary to describe the spectrum of  $d-d$  excitations. The EHCF approach was used as an appropriate method for this purpose. It allowed to reproduce the experimental data of the OA and EEL spectroscopy. In all the cases the reasonable agreement with the experiment was achieved by using larger cluster models without any special purpose parameterization process. The EHCF approach does not apply to the reactions in the coordination sphere of the transition metal ions since it does not take into account the electron correlation in the ligands. The natural modification of the EHCF approach was performed based on the effective Hamiltonian construction for a system consisting of the  $d$ -shell and active one-electron states of the ligands. This method can be applied to a wide range

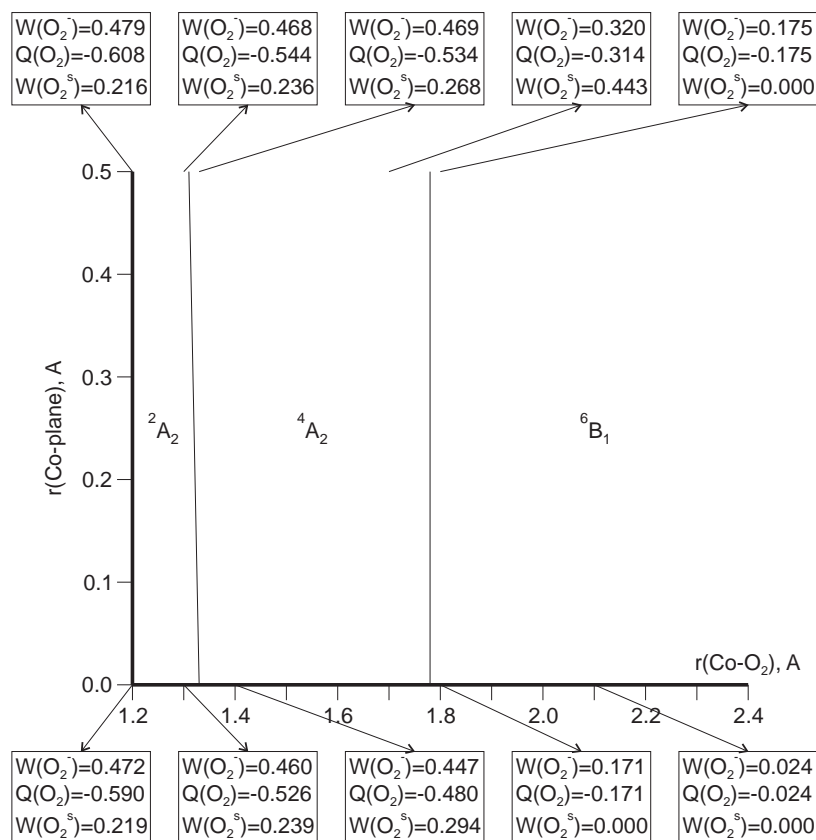


Fig. 5. Map for side-on adsorption of molecular oxygen on CoO:  $W(\text{O}_2^-)$ —weight of the anion form of the oxygen;  $W(\text{O}_2^s)$ —weight of the singlet form of the oxygen;  $Q(\text{O}_2^-)$ —charge on the oxygen.

of problems in the adsorption and catalysis. We studied the states of the atomic and molecular oxygen species adsorbed on the transition metal oxides and have found that the weights of singlet, charge-transfer and triplet states strongly depend on the structural characteristics of the adsorption and on the nature of the transition metal atom forming the oxide. The entanglement of the states of the *d*-shell and oxygen is of particular importance and the model based only on the effect of the TMO Coulomb field on the state of the oxygen seems to be oversimplified.

### Acknowledgments

This work has been performed with partial financial support of RFBR through the Grant 02-03-32087. Authors gratefully acknowledge valuable discussions with Prof. A.A. Levin. The authors are grateful to the referee for his instructions.

### References

- [1] G.K. Boreskov, in: J.R. Anderson, M. Boudart (Eds.), *Catalysis—Science and Technology*, Vol. 3, Springer, Berlin, Heidelberg, 1982, p. 39;
- [2] J.G. Bednorz, K.A. Müller, *Z. Phys. B—Condens. Matter* 64 (1986) 189–193.
- [3] P.A. Cox, *Transition Metal Oxides*, Clarendon Press, Oxford, 1992.
- [4] W.A. Harrison, *Electronic Structure and the Properties of Solids*, Freeman, San Francisco, 1990 (Chapter 19).
- [5] C.A. Morrison, *Crystal Fields for Transition-Metal Ions in Laser-Host Materials*, Springer, Berlin, 1992.
- [6] S. Hufner, *Adv. Phys.* 43 (1994) 183–356.
- [7] I. Pollini, A. Mosser, J.C. Parlebas, *Phys. Rep.* 355 (2001) 1–72.
- [8] N. Tsuda, K. Nasu, A. Yanase, K. Siratori, *Electronic Conduction in Oxides*, Springer, Berlin, Heidelberg, 1991.
- [9] J. Zaanen, G.A. Sawatzky, J. Allen, *Phys. Rev. Lett.* 55 (1985) 418–421.
- [10] H. Bethe, *Ann. Physik* 3 (1929) 133–208.
- [11] A. Zunger, in: H. Ehrenreich, D. Turnbull (Eds.), *Solid State Physics*, Vol. 39, Academic Press, Orlando, 1986, p. 276.
- [12] K.A. Kikoin, V.N. Fleurov, *Transition Metal Impurities in Semiconductors*, World Scientific, Singapore, 1994.
- [13] A.V. Soudackov, A.L. Tchougréeff, I.A. Misurkin, *Theor. Chim. Acta.* 83 (1992) 389–416.
- [14] R. McWeeny, *Methods of Molecular Quantum Mechanics*, 2nd Edition, Academic Press, London, 1992.
- [15] P.-O. Löwdin, *J. Math. Phys.* 3 (1962) 969–982.
- [16] A.V. Soudackov, A.L. Tchougréeff, I.A. Misurkin, *Int. J. Quantum Chem.* 58 (1996) 161–173.
- [17] V.F. Kiselev, O.V. Krylov, *Adsorption and Catalysis on Transition Metals and their Oxides*, Springer, Berlin, Heidelberg, 1989.

- [17] A.M. Tokmachev, A.L. Tchougréeff, *Khim. Fiz.* 18 (1999) 80–87 (in Russian) [*Chem. Phys. Rep.* 18 (1999) 163–177 (in English)].
- [18] A.V. Soudackov, K. Jug, *Int. J. Quantum Chem.* 62 (1997) 403–418.
- [19] A.M. Tokmachev, *Methods for electronic structure calculations of molecular systems with local electron groups*, Ph.D. Thesis, Moscow, 2003 (in Russian).
- [20] M.B. Darkhovskii, A.L. Tchougréeff, *Zh. Fiz. Khim.* 74 (2000) 360–367 (in Russian) [*Russ. J. Phys. Chem.* 74 (2000) 296–303 (in English)].
- [21] G. Wannier, *Phys. Rev.* 52 (1937) 191–197.
- [22] W. Kohn, *Phys. Rev.* 115 (1959) 809–821;  
W. Kohn, *Phys. Rev. B* 7 (1973) 4388–4398.
- [23] J. des Cloizeaux, *Phys. Rev.* 129 (1963) 554–566;  
J. des Cloizeaux, *Phys. Rev.* 135 (1964) A685–A697;  
J. des Cloizeaux, *Phys. Rev.* 135 (1964) A698–A707.
- [24] R. Hoffmann, *Solids and Surfaces: A Chemists View of Bonding in Extended Structures*, VCH Publishers, Berlin, NY, 1988.
- [25] P.S. Bagus, U. Wahlgren, *Mol. Phys.* 33 (1977) 641–650.
- [26] G.J.M. Janssen, W.C. Nieuwpoort, *Phys. Rev. B* 38 (1988) 3449–3458.
- [27] A. Freitag, V. Staemmler, D. Cappus, C.A. Ventrice, K. Al Shamery, H. Kuhlenbeck, H.-J. Freund, *Chem. Phys. Lett.* 210 (1993) 10–14.
- [28] A.L. Tchougréeff, *J. Mol. Catal.* 119 (1997) 377–386.
- [29] V. Staemmler, in: N. Russo, D.R. Salahub (Eds.), *Proceedings of the NATO Advanced Study Institute on Metal–Ligand Interactions: Structure and Reactivity*, Kluwer Academic Publishers, Dordrecht, Boston, London, 1996, p. 473.
- [30] R.A. Evarestov, *Quantum Chemical Methods in Solid State Theory*, Izd. LGU, Leningrad, 1982 (in Russian).
- [31] W.E. Garner, *Advances in Catalysis and Related Subjects*, Vol. IX, Academic Press, New York, 1957.
- [32] A. Nakamura, M. Tsutsui, *Principles and Applications of Homogeneous Catalysis*, Wiley-Interscience, New York, 1980.
- [33] A.L. Tchougréeff, *Int. J. Quantum Chem.* 57 (1996) 413–422.
- [34] A.L. Tchougréeff, *Int. J. Quantum Chem.* 58 (1996) 67–84.
- [35] R.B. Woodward, R. Hoffmann, *J. Amer. Chem. Soc.* 87 (1965) 395–397.
- [36] A.M. Tokmachev, A.L. Tchougréeff, I.A. Misurkin, *Int. J. Quantum Chem.* 84 (2001) 99–109.
- [37] O. Gunnarson, K. Schönhammer, *Phys. Rev. B* 31 (1985) 4815–4834.
- [38] J. Paldus, in: H. Eyring, D. Henderson (Eds.), *Theoretical Chemistry, Advances and Perspectives*, Vol. 2, Academic Press, New York, 1976, p. 131.
- [39] A.V. Soudackov, A.L. Tchougréeff, I.A. Misurkin, *Zh. Fiz. Khim.* 68 (1994) 1256–1264 (in Russian) [*Russ. J. Phys. Chem.* 68 (1994) 1135 (in English)].
- [40] M.G. Razumov, A.L. Tchougréeff, *Zh. Fiz. Khim.* 74 (2000) 87–93.
- [41] R. Newman, R.M. Chrenko, *Phys. Rev.* 114 (1959) 1507–1513.
- [42] G.W. Pratt Jr., R. Coelho, *Phys. Rev.* 116 (1959) 281–286.
- [43] M. Haßel, H. Kuhlenbeck, H.-J. Freund, S. Shi, A. Freitag, V. Staemmler, S. Lütkehoff, M. Neumann, *Chem. Phys. Lett.* 240 (1995) 205–209.
- [44] G.K. Borekov, *Kinet. Katal.* 8 (1967) 1020–1033.
- [45] A. Bielanski, M. Najbar, *J. Catal.* 25 (1972) 398–406.
- [46] A. Bielanski, J. Haber, *Catal. Rev.* 19 (1979) 1–41.
- [47] C. Naccache, *Chem. Phys. Lett.* 11 (1971) 323–325.
- [48] V.A. Shwets, V.B. Kazanskii, *J. Catal.* 25 (1972) 123–130.
- [49] C.W. Patterson, W.G. Harter, *Phys. Rev. A* 15 (1977) 2372–2379.
- [50] M.B. Darkhovskii, M.G. Razumov, I.V. Pletnev, A.L. Tchougréeff, *Int. J. Quantum Chem.* 88 (2002) 588–605.
- [51] I.D. Mikheikin, I.K. Vorontsova, I.A. Abronin, *Int. J. Quantum Chem.* 88 (2002) 489–495.